

Dynamic analysis of the scale-up of fluidized beds

Tahmasebpoor, M.; Zarghami, R.; Sotudeh-Gharebagh, R.; van Ommen, J. R.; Mostoufi, N.

DOI

[10.1016/j.appt.2017.07.014](https://doi.org/10.1016/j.appt.2017.07.014)

Publication date

2017

Document Version

Final published version

Published in

Advanced Powder Technology

Citation (APA)

Tahmasebpoor, M., Zarghami, R., Sotudeh-Gharebagh, R., van Ommen, J. R., & Mostoufi, N. (2017). Dynamic analysis of the scale-up of fluidized beds. *Advanced Powder Technology*, 28(10), 2621-2629. <https://doi.org/10.1016/j.appt.2017.07.014>

Important note

To cite this publication, please use the final published version (if applicable). Please check the document version above.

Copyright

Other than for strictly personal use, it is not permitted to download, forward or distribute the text or part of it, without the consent of the author(s) and/or copyright holder(s), unless the work is under an open content license such as Creative Commons.

Takedown policy

Please contact us and provide details if you believe this document breaches copyrights. We will remove access to the work immediately and investigate your claim.



Original Research Paper

Dynamic analysis of the scale-up of fluidized beds

M. Tahmasebpour^a, R. Zarghami^{b,*}, R. Sotudeh-Gharebagh^b, J.R. van Ommen^c, N. Mostoufi^b^a Department of Chemical & Petroleum Engineering, University of Tabriz, P.O. Box 5166616471, Tabriz, Iran^b Multiphase Research Systems Lab., School of Chemical Engineering, College of Engineering, University of Tehran, P.O. Box 11155/4563, Tehran, Iran^c Delft University of Technology, Department of Chemical Engineering, Van der Maasweg 9, 2629 HZ Delft, The Netherlands

ARTICLE INFO

Article history:

Received 10 September 2016

Received in revised form 11 May 2017

Accepted 18 July 2017

Available online 29 July 2017

Keywords:

Fluidized bed

Scale-up

Recurrence quantification analysis

Pressure fluctuations

Entropy

ABSTRACT

A method is developed for hydrodynamics scale-up of gas-solid fluidized beds based on recurrence quantification analysis of nonlinear time series of pressure fluctuations. This method is an improvement of the previous method by including the entropy of pressure fluctuations to the list of scale-up parameters. Experiments were carried out at varying conditions, e. g., bed diameter (5, 9, 15, 40 and 80 cm ID), particle size (150, 300, 400 and 600 μm), bed height at aspect ratios (1, 1.5 and 2) and superficial gas velocities (ranging 0.1 to 1.7 m/s) to identify the main parameters that influence the dynamics and to develop a general interpretation of the analysis results. By investigation of the effect of operating parameters on entropy, a quantitative empirical correlation is proposed for including the entropy in the scale-up parameters. It was shown that this correlation improves the Glicksman's method for the scale-up of fluidized beds.

© 2017 The Society of Powder Technology Japan. Published by Elsevier B.V. and The Society of Powder Technology Japan. All rights reserved.

1. Introduction

Scale-up of fluidized beds has always been an obstacle in wide-spread use of these reactors in industry. This difficulty arises from the fact that the hydrodynamics of fluidized beds is very complex and, especially, the effect of bed diameter is still not very well understood. Proper description of the hydrodynamics of gas-solid fluidized beds is difficult since fluidized beds are a heterogeneous mixture of gas and solids exhibiting a liquid-like behavior [1]. Considering that scale-up deals with the hydrodynamics, having no detailed understanding of the hydrodynamics of fluidized beds is believed to be one of the key reasons for the difficulties encountered in design and scale-up of fluidized beds [2]. Therefore, detailed understanding of their hydrodynamics can definitely improve the scaling. The hydrodynamics of gas-solid fluidized beds are usually studied using time series evaluation of the measured signals [3,4]. Different time series signals can be used for studying the bed hydrodynamics such as pressure fluctuations [3,5,6], bed vibration [7–9], acoustic emissions [10–12] and local porosity [13]. However, pressure fluctuation measurements have some advantages that make them suitable for many practical applications. These advantages are ease of measurement and inclusion of the effect of various dynamic phenomena, such as bubble hydrodynamics, occurring in the bed [3,14].

The hydrodynamics of a fluidized bed are non-linear, and could be even considered chaotic, although the latter is being debated [15]. A way to describe the state of such a system is to project the variables governing the system into its multi-dimensional state space [14]. Recently, a new technique based on the nonlinearity of the dynamics, called recurrence quantification analysis (RQA), has been developed [16]. The concept of the RQA, which relies on the presence of recurring/deterministic structures underlying the data, is a basic property of dynamical systems, which can be exploited to describe the behavior of the system in the phase space. Tahmasebpour et al. [17,18]) and Babaei et al. [19] demonstrated that RQA is a powerful tool to study fluidization hydrodynamics.

In the present study, nonlinear time series analysis technique based on RQA is explored to characterize the hydrodynamics of gas-solid fluidized beds, focusing on improving the scale-up procedure. It will be shown that how nonlinear RQA method can help to improve the Glicksman's non-dimensional scaling method [20] by identifying the most relevant dimensionless group as dictated by the RQA. The Shannon entropy, one of the quantitative concepts of the RQA method, is introduced to quantify the fluidized bed hydrodynamics representatively, based on measured pressure fluctuation data. The entropy is related to superficial gas velocity, size of particles, settled bed height and bed diameter. Then, this modeled entropy will be used to establish hydrodynamic similarities between two fluidized beds of diameters 9 and 15 cm ID.

* Corresponding author.

E-mail address: rzarghami@ut.ac.ir (R. Zarghami).

Nomenclature

a_j	approximate sub-signal	L	settled bed height, m
d	dimension of the system	N	length of the time series
d_s	particle size, μm	$p(l)$	number of diagonal lines with length of l
D	bed diameter, m	$R_{i,j}$	recurrence plot matrix
D_j	detail sub-signal	T	time, s
E_j^a	energy of approximation sub-signal at level j , Pa^2	U_0	superficial gas velocity, m/s
E_j^D	energy of detail sub-signal at level j , Pa^2	U_{mf}	minimum fluidization velocity, m/s
ENT	entropy, bits/cycle	$x(i)$	pressure time series, Pa
f	frequency, Hz	x_i	i -th point of space state trajectory
f_s	sampling frequency, Hz	x_j	j -th point of space state trajectory
G_s	solids circulation flux, kg/s.m^2		
i	counter		
j	complex number		
j	wavelet decomposed information level		
k	time lag coefficient		
l	length of a diagonal line		
l_{min}	predefined minimal length of diagonal lines		
		<i>Greek letters</i>	
		ε	threshold radius
		ψ	mother wavelet function
		Θ	Heaviside function
		ρ_s	particle density, kg/m^3
		ρ_f	gas density, kg/m^3
		φ	particle sphericity

2. Experiments

Experiments were carried out in 5 different gas–solid fluidized beds in the University of Tehran and Delft University of Technology. Experimental conditions are summarized in Table 1. Air at room temperature was supplied to the bed through a distributor and its flow rate was controlled by a mass flow controller. A cyclone, placed at the column exit, would return the entrained solids back to the bed. Various initial aspect ratios of solids ($L/D = 1, 1.5$ and 2) were used in experiments and the superficial gas velocity was varied in the range of 0.1 – 1.7 m/s. Sand particles (Geldart B) with a Sauter mean diameter of $150, 300, 400$ and $600 \mu\text{m}$ and a particle density of 2700 kg/m^3 were used in the experiments.

Measured pressure signals were band-pass filtered at lower cut-off frequency and upper cut-off Nyquist frequency. The filtered signals were then amplified and sent to a data acquisition board system. Johnsson et al. [3] and van der Stappen et al. [21] recommended that the sampling frequency within the range of 50 – 100 times the average cycle frequency (typically between 100 and 600 Hz) is required for nonlinear evaluation of pressure fluctuations in bubbling fluidized beds. Selected sampling frequencies, lower cut-off and upper cut-off Nyquist frequencies and number of data points collected in each fluidized bed are shown in Table 1.

3. Method of analysis

Methods of data analysis used in this work are briefly described below.

3.1. Recurrence plot

The recurrence plot (RP) is a graphical explanation of the dynamics of a system [22]. A RP provides a qualitative picture of

the correlations between the states of a time series over all available time-scales. It is a 2-dimensional plot which is mathematically expressed as:

$$R_{i,j} = \Theta(\varepsilon - \|x_i - x_j\|) \quad i, j = 1, 2, 3, \dots, N \quad (1)$$

where N is the number of considered states, $x_i, x_j \in R^d$ represent the i -th and j -th points of the d -dimensional state space trajectory, $\| \cdot \|$ represent the norm, ε is a threshold distance and Θ is the Heaviside function. The RP is obtained by plotting the recurrence matrix, Eq. (1); if $R_{i,j} = 1$ it is considered as a recurrence point and appears as a black dot at the coordinate (i, j) , if $R_{i,j} = 0$ it is shown as a white dot. The RP can be constructed without embedding [23]. Therefore, in the present work, the embedding dimension was considered to be 1.

3.2. Recurrence quantification analysis

The RQA is developed for quantifying different graphical structures of RPs. Recurrence parameters describe distribution of various structures in the RP, including single dots, diagonal lines and vertical or horizontal lines [16]. Entropy (ENT) in the RQA is the Shannon information entropy of the probability distribution of the diagonal line lengths l :

$$ENT = - \sum_{l_{min}}^N p(l) \log_2 p(l) \quad (2)$$

The probability distribution of the diagonal line lengths $p(l)$ is defined as:

$$p(l) = P(l)/N_l \quad (3)$$

where $P(l)$ is the frequency distribution of the lengths l of the diagonal line in the RP and N_l is the number of diagonal lines.

Table 1
Experimental conditions.

Bed	Diameter (cm)	University	Particle size (μm)	Density (kg m^{-3})	Sampling frequency (Hz)	Lower cut-off frequency (Hz)	Upper cut-off frequency (Hz)	Data points
Bed 5	5	Tehran	150–300–600	2700	400	0.1	200	1,200,000
Bed 9	9	Tehran	150–300–600	2700	400	0.1	200	1,200,000
Bed 15	15	Tehran	150–300–600	2700	400	0.1	200	1,200,000
Bed 40	40	Delft	400	2700	80	Off	40	262,144
Bed 80	80	Delft	400	2700	200	Off	60	720,896

Entropy is expressed in bits/cycle and quantifies the unpredictability and complexity of a system. Entropy is zero for a periodic system (all diagonal lines are of equal length) and assumes a large value in a chaotic (complex) system [16]. Entropy has often been used to characterize fluidized bed hydrodynamics in literature. Therefore, it was also considered in the present study as a characterization tool since it is sensitive to changes in operating conditions.

3.3. Discrete wavelet transform

Compared to other methods of analysis of signal in the frequency domain, the wavelet transform (WT) provides more flexibility in the time-frequency representation of a signal by allowing the use of variable sized windows [7,24]. In fact, the WT can provide precise frequency information at both low and high frequencies. The discrete wavelet transform (DWT) is defined as:

$$DWT(j, k) = \frac{1}{\sqrt{|2^j|}} \int x(t) \psi\left(\frac{t - k \cdot 2^j}{2^j}\right) dt \quad (4)$$

In the present work, the procedure developed by Mallat [24] was followed in which the passes signal through a series of low-pass and high-pass pairs of filters called quadrature mirror filters. At each step of the decomposition process, the frequency resolution is doubled through filtering and the time resolution is halved through down-sampling. The sub-signals (decomposed) are then composed of the approximation sub-signal $a_j(t)$ and the detail sub-signal $D_j(t)$. Thus, the original signal $x(t)$ can be reconstructed from the sub-signals of different scales:

$$x(t) \approx a_j(t) + D_j(t) + D_{j-1}(t) + \dots + D_1(t) \quad (5)$$

The approximation component of the signal contains information of the low frequency of the original signal and the detail component corresponds to information of the high frequency of the original signals [25].

Energies of approximation, $a_j(t)$, and detail, $D_j(t)$, sub-signals are defined as:

$$E_j^a = \sum_{t=1}^N |a_j(t)|^2 \quad (6)$$

$$E_j^D = \sum_{t=1}^N |D_j(t)|^2 \quad (7)$$

Total energy of the original signal $x(t)$ can be calculated by summing energies of the sub-signals as follows [3,25]:

$$E = \sum_{t=1}^N |x(t)|^2 = E_j^a + \sum_{j=1}^J E_j^D \quad (8)$$

4. Results and discussion

Three different hydrodynamic structures i.e., micro-, meso- and macro-structures) can be recognized in a fluidized bed [26]. The macro structures have high amplitude and low frequencies and are likely include large scale phenomena such as large bubbles and bed surface oscillation. The meso structures can be contributed to clusters and small bubbles which have lower amplitude and higher frequencies. The micro structures are of high frequencies; they might originate from impacts of solid particles, their motion and also include noise in the fluidized bed [25,27]. Please note that associating phenomena with certain frequency ranges is not straightforward, and sometimes still subject of discussion [14]. Tahmasebpour et al. [18] showed that, in a fluidized bed of 15

cm diameter, micro-, meso- and macro-structures can be represented by frequencies in the range of 25–200 Hz, 3.125–25 Hz and 0–3.125 Hz, respectively.

Fig. 1 shows relative energies of macro and meso structures (with reference to the total energy) of the pressure fluctuations measured in three small bed sizes for 300 μm sand particles and $L/D = 2$. The probe was placed in these beds in such a way that the ratio of the probe position to the settled height of solids was the same. As shown in Fig. 1, while the relative energy of the macro structures initially increases by increasing the gas velocity and then gradually decreases, the relative energy of meso structures shows an opposite trend. Macro structures have the most energy in the bubbling fluidized bed. In addition, the relative energy of structures in these three beds for both structures is quite similar. Although it might be expected that the bed size would affect the contribution of structures due to change in the wall effect for different bed sizes, Fig. 1 does not reflect this trend which reveals that the wavelet analysis method may not be sensitive enough to the bed scale. It should be noted that all the Glicksman's dimensionless numbers (ρ_s/ρ_f , u_0/u_{mf} , $G_s/\rho_s u_0$, L/D , bed geometry, ϕ , PSD) are the same in the three beds of Fig. 1. In other words, Glicksman's method [20] predicts a similar hydrodynamic behavior for these beds based. Obviously, the wall effect decreases by increasing the bed diameter such that it vanishes beyond a certain diameter. However, the wall effect cannot be neglected in small diameter beds since particle/gas contact with the wall affects particle-gas interactions [1]. In fact, Fig. 1 shows that the wavelet analysis may not identify all differences in the hydrodynamic of these small beds.

Tahmasebpour et al. [28] showed that the RP is capable of recognizing various structures in a fluidized bed. Therefore, these plots were used in this work to various bed sizes to distinguish the wall effect. RPs for macro and meso structures, as well as the corresponding raw signal, measured for 300 and 400 μm sand particles in four bed sizes (5, 15, 40 and 80 cm) at superficial gas velocity of 0.7 m/s are shown in Fig. 2a–d. As can be seen in these figures, structures and their contribution are different in beds with different sizes. Fig. 2a and b illustrates that RP of the raw signal is very similar to that of the macro-structure in small beds (5 and 15 cm). This is consistent with the result shown in Fig. 1. Gradually, by increasing the bed diameter, the RP of the raw signal becomes more similar to that of the meso-structure. As shown in Fig. 2c and d, RP of the raw signal resembles that of the meso-structure for larger beds (40 and 80 cm). Therefore, it can be concluded that meso structures become dominant by increasing the size of the bed while macro structures are more important in small-

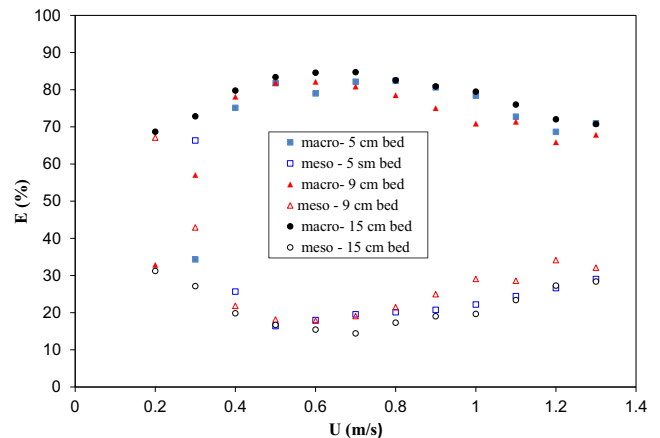


Fig. 1. Relative energies of macro and meso structures in the pressure signals measured in three beds (5, 9 and 15 cm) for 300 μm sand particles and $L/D = 2$.

ler beds. In other words, the macro structure is the dominant structure in small beds while by increasing size of the bed, the contribution of meso structures increases such that in large beds it becomes the dominant structure of the bed. This qualitative result should be discussed more quantitatively by the RQA method.

Dependence of entropy on the operating conditions of fluidization was also investigated. The entropy of a bed of 300 μm sand particles in small beds (5, 9 and 15 cm ID) and 400 μm sand particles in large beds (40 and 80 cm ID) is presented in Fig. 3. As can be seen in this figure, entropy of the system in larger beds is greater than that in smaller beds. This is consistent with the trend shown in Fig. 2 for meso structures. Moreover, Fig. 3 reveals that there is no meaningful difference between entropies of 40 and 80 cm ID beds. Therefore, it can be concluded that by increasing the bed diameter, the role of meso structures increases in the hydrodynamics of the bed such that beyond a certain diameter they become the dominant structure in the bed. This certain diameter is considered as the scaling diameter in the present study, beyond which the hydrodynamics of the bed becomes independent of the bed diameter. In other words, wall effects can be neglected in beds larger than the scaling diameter. While wavelet analysis cannot identify the wall effects in small beds (see Fig. 1), the wall effects can be characterized by entropy (Fig. 3). In addition, Fig. 3 shows that while the entropy decreases at low gas velocities, it is almost inde-

pendent of the gas velocity in the bubbling regime (0.5–1 m/s in this work).

Fig. 4a shows the entropy, averaged over the ranges gas velocity indicated on the figure, versus the bed diameter at various operating conditions. This figure illustrates that the entropy increases rapidly as the bed diameter increases. This sharp change at small bed diameters can be attributed to the wall effect, as mentioned in discussions of Fig. 3. However, it can be seen in Fig. 4a that at large bed diameters, the entropy reaches an approximately constant value. Therefore, in order to confidently estimate the hydrodynamic parameters at an industrial scale fluidized bed, it is necessary to do the measurements where hydrodynamic parameters do not change with increasing the bed diameter [1,29]. Alternatively, the measurements can be done in small beds, then, corrected by knowing the relationship between the parameter and bed diameter. Based on Fig. 4a, it can be suggested that the entropy to be used as a parameter for studying the scale effect in fluidized beds and that the required hydrodynamic measurements to be carried out in a bed with diameter at which the entropy has levelled off. It is worth noting in Fig. 4a that entropy is higher in a bed of smaller particles. Effect of particle size on the entropy of the fluidized bed was also investigated by Tahmasebpour et al. [28] who showed this trend more clearly. As a result, the scaling diameter (the bed diameter at which the entropy reaches a constant) is

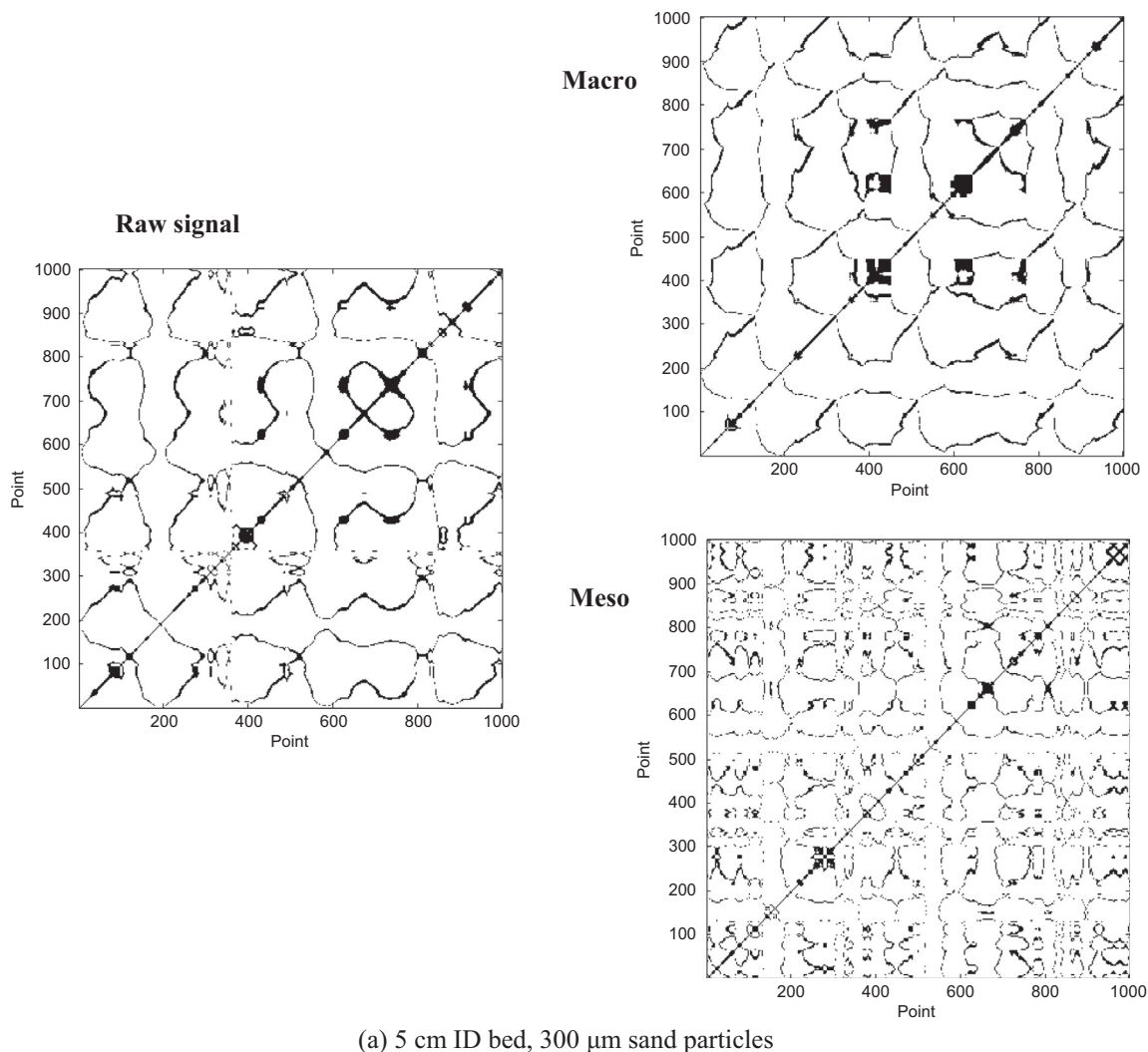


Fig. 2. Recurrence plots for macro and meso structures and raw signal measured at $L/D = 1$ and superficial gas velocity of 0.7 m/s for (a) 5 cm ID bed, 300 μm sand particles (b) 15 cm ID bed, 300 μm sand particles (c) 40 cm ID bed, 400 μm sand particles (d) 80 cm ID bed, 400 μm sand particles.

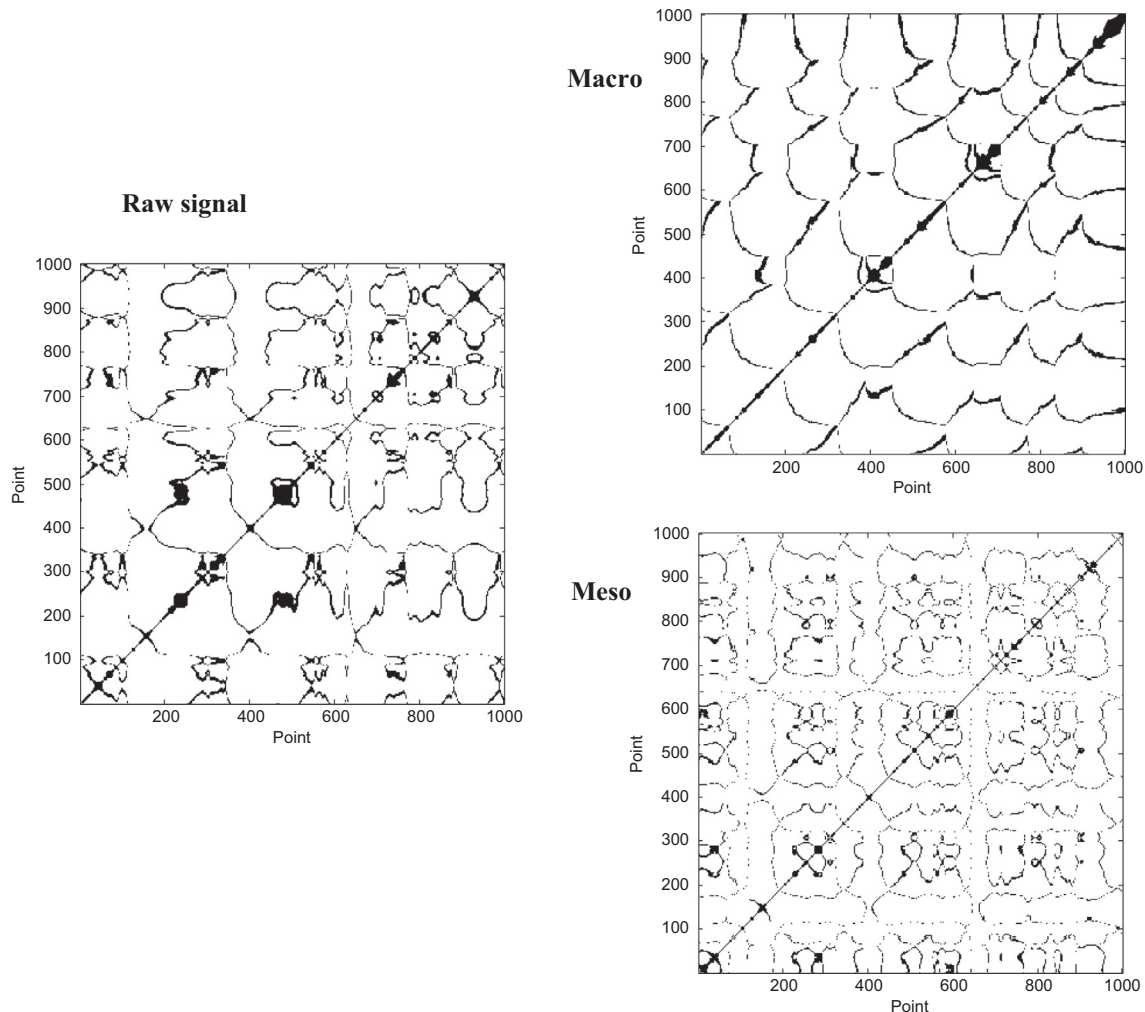
(b) 15 cm ID bed, 300 μm sand particles

Fig. 2 (continued)

smaller in a bed of smaller particles. Therefore, in order to combine the effect of bed size and particle size, the entropy is also plotted versus the ratio of bed diameter to particle size in Fig. 4b. In the following section, the trend in this figure was used for developing a correlation to be used for scale up of fluidized beds.

5. A correlation for entropy

In this section, the entropy is quantitatively related to design parameters; i.e., fluidization conditions (superficial gas velocity, settled bed height), particle properties (particle size, minimum fluidization velocity) and bed diameter. In the present study, these parameters are changed in the following range: bed diameter (5, 9, 15, 40 and 80 cm ID), particle size (150, 300, 400 and 600 μm), aspect ratio (1, 1.5 and 2) and superficial gas velocity (ranging in different levels according to bed size and particle size). It is worth mentioning that effect of all these parameters on the entropy has been previously investigated in details and compared with literature by Tahmasebpour et al. [28]. With more than 200 data points, entropy can be correlated to the above mentioned operating variables by the following correlation:

$$ENT = a \left(\frac{U_0 - U_{mf}}{U_{mf}} \right)^b \frac{D^c}{L^d d_s^e} = 1.2 \left(\frac{U_0 - U_{mf}}{U_{mf}} \right)^{0.045} \frac{D^{1.27}}{L^{0.43} d_s^{0.46}} \quad (9)$$

The fitting constants (a , b , c , d and e) were obtained by MATLAB optimization toolbox. It should be noted that this correlation covers the rising section of Fig. 4a and b and can be used for diameters smaller than the scaling diameter. Fig. 5 illustrates the parity plot of measured entropies against those calculated from Eq. (9) and these points are shown in blue¹ in Fig. 5. This means that some of entropy data were not used in the fitting process, hence had no contribution in calculating the fitting constants. The remained 20% data points were used for validating the correlation. These data are shown with red markers in Fig. 5. Based on the fact that the main data points are uniformly distributed around the unity line and also since validation points show almost the same distribution, it can be concluded that the correlation may satisfactorily predict the real values.

6. Proposed scale-up procedure

Entropy characterizes all the relevant information about the behavior of a system [16]. In fact, it characterizes the rate of information loss in a system and is a quantitative measure for

¹ For interpretation of color in Fig. 5, the reader is referred to the web version of this article.

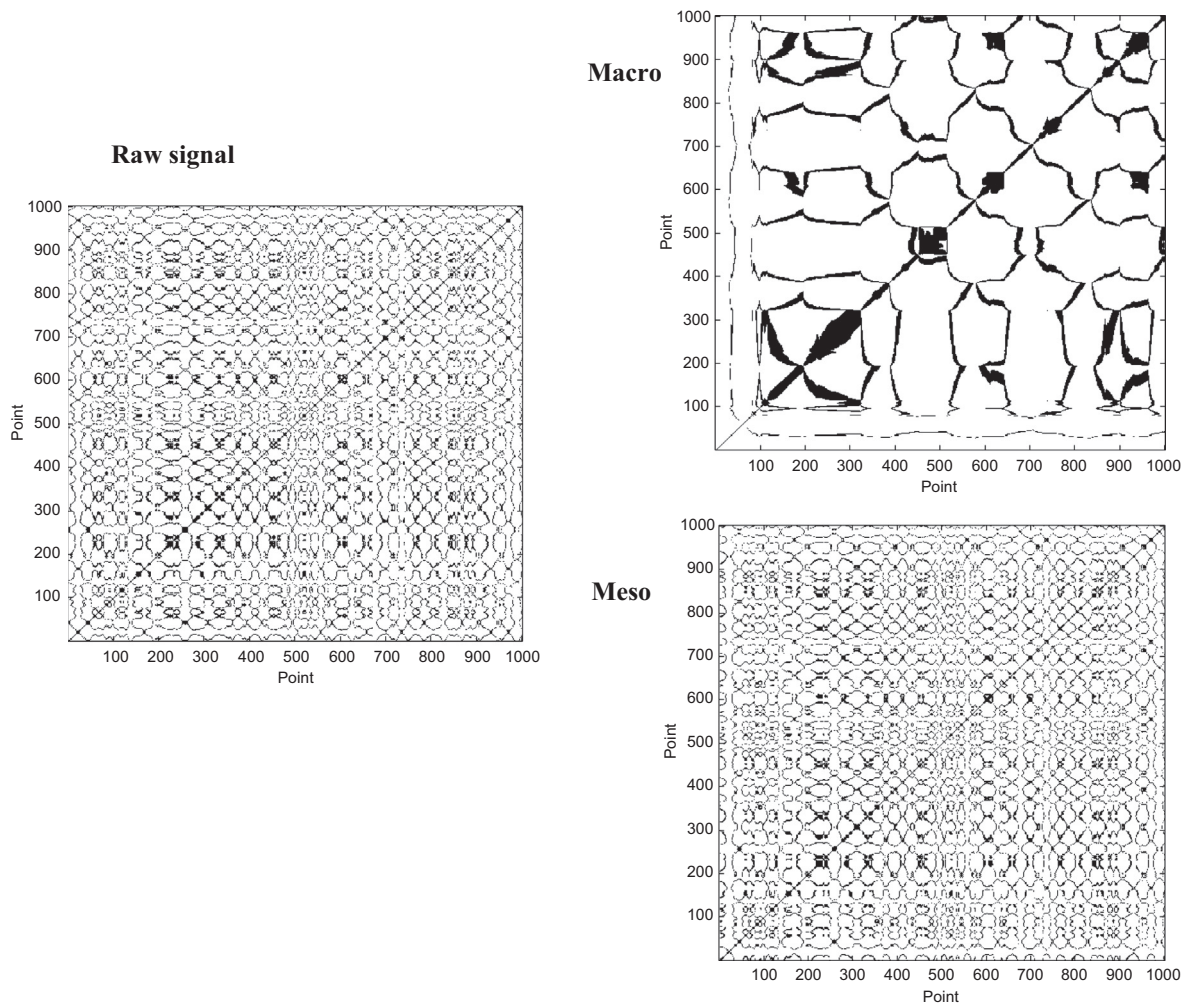
(c) 40 cm ID bed, 400 μm sand particles

Fig. 2 (continued)

predictability of a dynamical process. Entropy is preferred as a characterization tool since it provides additional information about bubble related time scales, is more sensitive to changes in operating conditions and is more robust and better reproducible [2]. If a fluidized bed is to be scaled properly, the prototype and the scaled bed should have the same entropy. In other words, the same information should be carried from the prototype to the scaled bed during the scale-up process. The so-called simplified set of dimensionless groups in the scale-up method of Glicksman is:

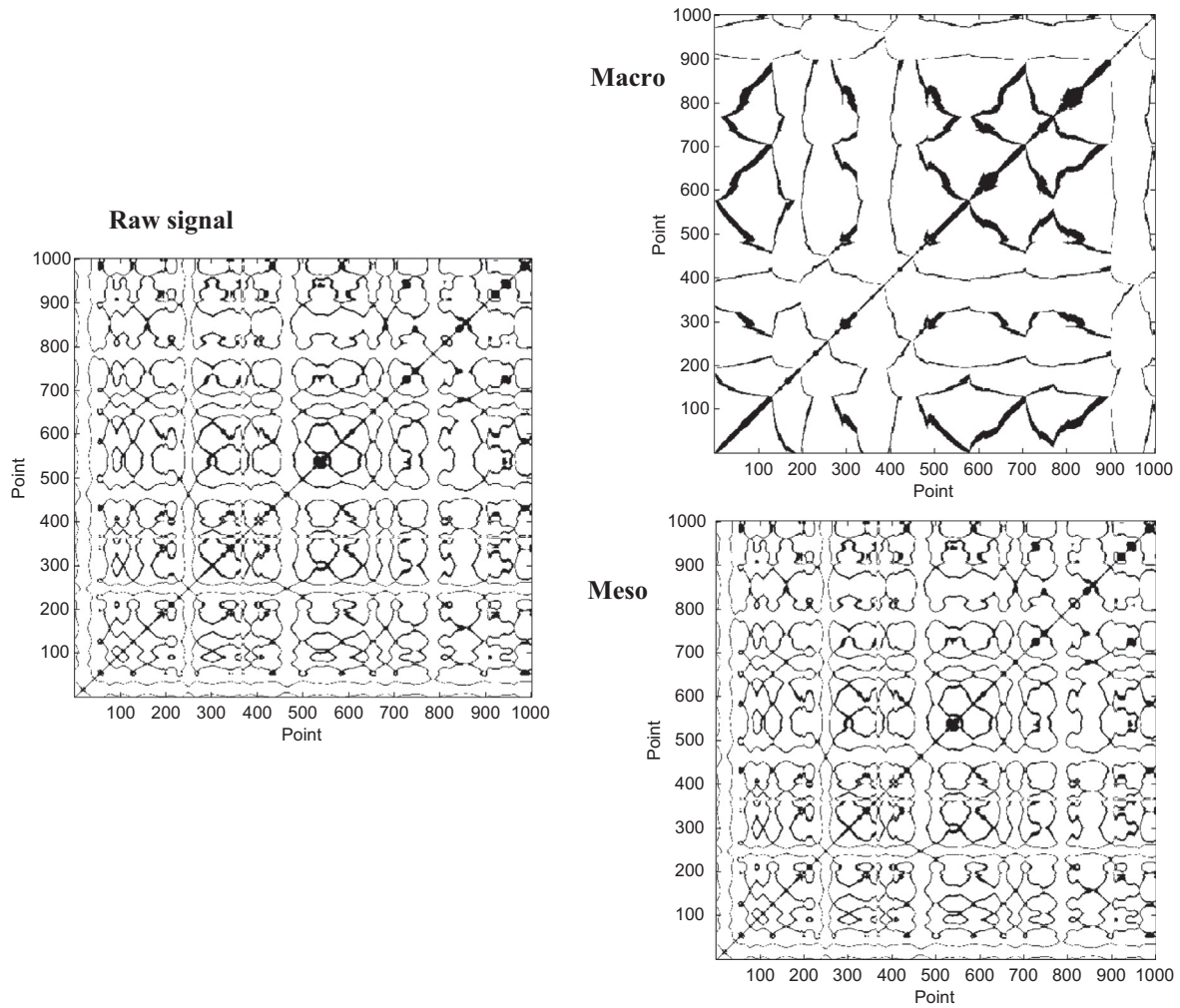
$$\frac{\rho_s}{\rho_f}, \frac{u_0}{u_{mf}}, \frac{G_s}{\rho_s u_0}, \frac{L}{D}, \text{ bed geometry}, \phi, \text{ PSD}$$

It should be noted that solids circulation flux is negligible in bubbling and turbulent fluidized beds. Sphericity of particles and particle size distribution should be the same in different scales. It is worth noting that the sphericity of sand particles used in this study were approximately equal. According to the Glicksman's method, the hydrodynamic state of both prototype and scaled should be the same if all abovementioned dimensionless numbers are the same for both beds. Nevertheless, it was shown here and also Tahmasebpour et al. [28] found that entropy of the bed changes even when all these dimensionless parameters are kept constant. This means that although the dimensionless groups proposed by Glicksman are kept constant, the two beds may not

be necessarily in the same hydrodynamic state. Therefore, entropy is suggested to be used for assessing the dynamical similarity between two scaled fluidized beds. Therefore, L/D in the Glicksman's simplified set is replaced by entropy in this work owing to the fact that it does not change with the gas velocity in the bubbling regime (see Fig. 3). On the other hand, the entropy can be different for beds with similar L/D [28]. This shows that the entropy has more dynamical information about the system than L/D . Therefore it can be concluded that L/D may not be an appropriate scale-up parameter for fluidized beds and it can be replaced by entropy. In other words, it is proposed in this work to replace L/D in the Glicksman's so-called 'simplified set' with the entropy. Based on the above discussion, it can be proposed to use the following set of dimensionless groups for the of gas-solid fluidized beds:

$$\frac{\rho_s}{\rho_f}, \frac{u_0}{u_{mf}}, \frac{G_s}{\rho_s u_0}, ENT, \text{ bed geometry}, \phi, \text{ PSD}$$

As an example, the 9 cm ID bed used in this work was scaled up to 15 cm ID bed by the two above mentioned methods. The operating conditions are given in Table 2. The scaling parameters (i.e., type and size of particles, type of gas, superficial gas velocity and geometry of both columns) are kept constant in this example. The bed height at rest was considered to be equal to the bed diameter in the smaller bed ($L=9$ cm). Therefore, based on the



(d) 80 cm ID bed, 400 μm sand particles

Fig. 2 (continued)

Gliksman’s method, the bed height in the scaled reactor should be 15 cm. Nevertheless, based on the new method which is based on entropy, according to Eq. (8), it is necessary to keep the ratio $D^{1.27}/L^{0.43}$ constant in order to keep the entropy the same in both scales. To do so, the entropy is determined first in the 9 cm ID bed. Then, by keeping this entropy the same, the initial bed height in the scaled bed (15 cm ID) is found which gives the initial bed height of about 30 cm for the scaled bed.

Fourier transform analysis was employed to compare the hydrodynamic state of these two scaled beds. Fig. 6 illustrates the frequency spectra of the pressure fluctuations measured in these two beds at the superficial gas velocity of 0.6 m/s. Pressure signals were divided into 8 non-overlapping windows of 8192 samples and then the frequency spectrum was obtained by the method of Welch method and Hanning window [30]. As can be seen in this figure, the dominant frequency of the pressure fluctuations lies between 0 and 10 Hz with a maximum at about 1.5–2.5 Hz. This peak corresponds to the macro structures of the bed. Fig. 6 reveals that when the entropy-based scaling rule is applied, both beds behave more similar from the hydrodynamics point of view since the power of the frequency spectra, as well as their width, are in a similar range. Considering that the main frequencies of the fluidized bed are mostly related to larger structures (like bubbles), it can be concluded that the macro structures have more

portions in the prototype (9 cm ID, $L/D = 1$) and the scaled bed (15 cm ID, $L/D = 2$). This fact can be also confirmed by the entropy of the signal. Fig. 7 shows the measured entropy for two cases of scal-

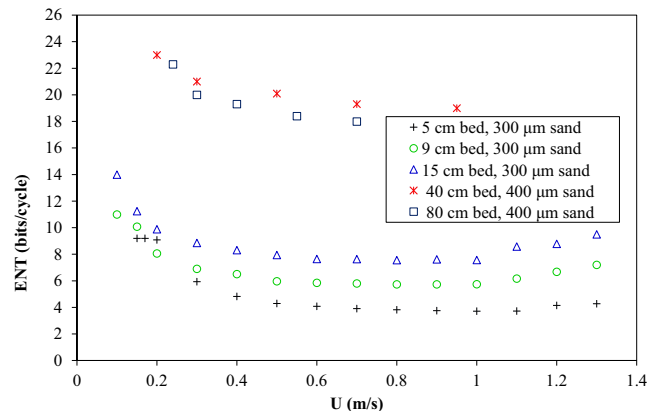


Fig. 3. Entropy of the pressure signals measured in 5, 9 and 15 cm ID beds for 300 μm sand particles and in 40 and 80 cm ID beds for 400 μm sand particles, $L/D = 1$.

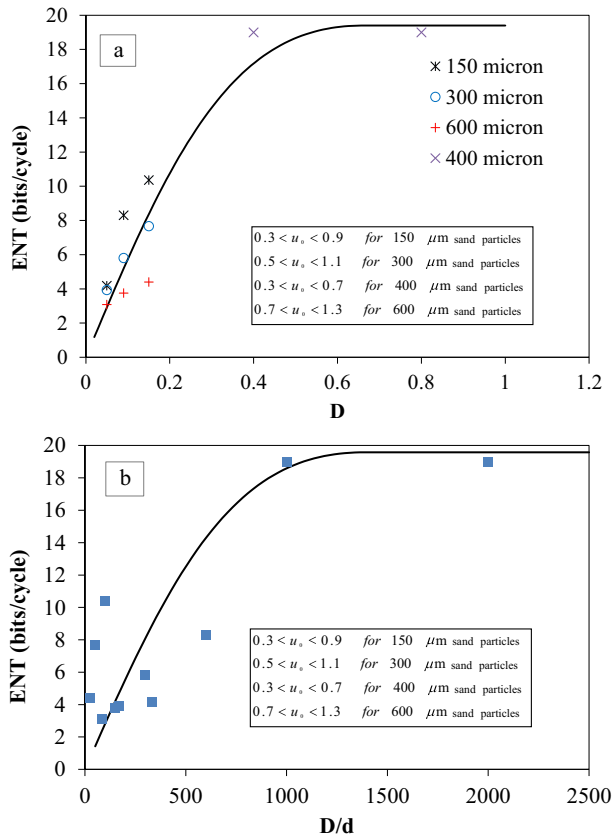


Fig. 4. Average entropy (bits/cycle) of the pressure signals measured in different conditions versus (a) bed diameter (D) and (b) bed diameter to particle size ratio (D/d).

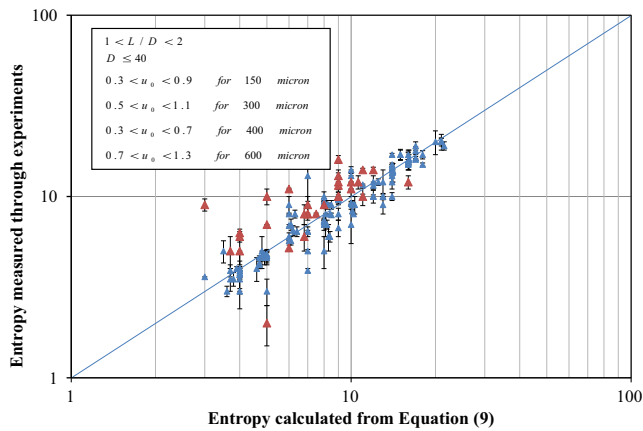


Fig. 5. Correlation between measured entropies and the model correlation [Eq. (9)].

ing mentioned in Table 2. It can be seen in this figure that the scaling is very well done when the entropy-based scaling rule is applied and both beds behave the same from the hydrodynamics point of view since the when the entropy-based scaling rule is applied entropy of the prototype (9 cm ID, $L/D = 1$) is very close to the entropy of the scaled bed (15 cm ID, $L/D = 2$). However, the entropy is very different for the two beds when they are scaled by the Glicksman’s method (15 cm ID, $L/D = 1$). This shows that the system complexity is a key parameter that should not be ignored in the scaling rules. Fig. 7 relies on the fact that if two beds are properly scaled, the information in both systems would remain the

Table 2
Operating conditions used in the scaling example.

	Bed 9	Bed 15	
		Glicksman’s method	Entropy based method
d_s (μm)	150	150	150
u_0 (m/s)	0.5–0.9	0.5–0.9	0.5–0.9
u_{mf} (m/s)	0.0287	0.0287	0.0287
ρ_s (kg/m ³)	2700	2700	2700
ρ_f	Same	Same	Same
PSD	Same	Same	Same
G_s	Same	Same	Same
L	9	15	30
D	9	15	15

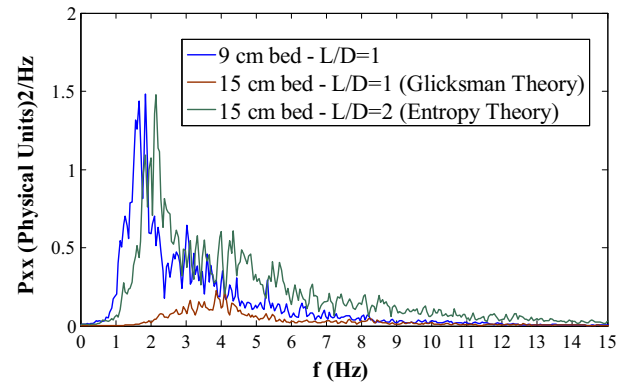


Fig. 6. The power spectrum estimation of the measured pressure fluctuations at superficial gas velocity of 0.6 m/s according to the data in Table 2.

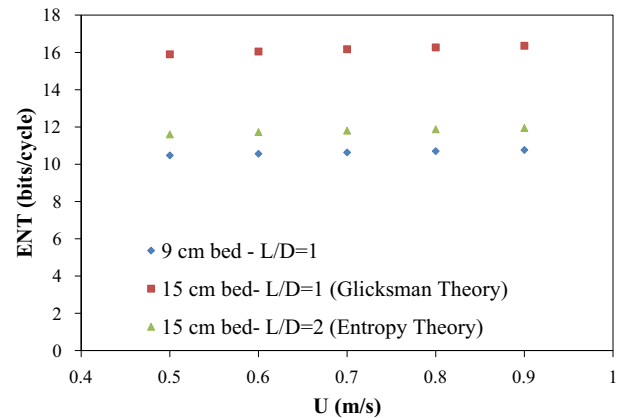


Fig. 7. Entropy (bits/cycle) of the system according to the data in Table 2.

same. In other words, the entropy should be considered as one of the major parameters in the scaling of fluidized beds for reach the same hydrodynamic state in different scales. In earlier work, we showed that the entropy expressed in bit/s often gave the same information as the average frequency [15] or the average cycle frequency [14]. It is important to note that here we employed the entropy expressed in bits/cycle (i.e., normalized with respect to time scale), which apparently contains information in addition to the main time scale.

7. Conclusions

It was shown that the RQA analysis is a valuable tool for understanding the hydrodynamics and scaling-up of fluidized beds. The

most useful parameter in the scale-up is the entropy of the system which can be evaluated from a time series of a characteristic system variable, such as pressure fluctuations. The entropy can be regarded as a measure of the complexity of the system.

The following conclusions were drawn from the present investigation:

- Contribution of meso structures in the hydrodynamics increases by increasing the bed size. In other words, by decreasing the wall effect, which happens by increasing the bed size, entropy of the system increases until the scaling diameter, beyond which it becomes constant. While it was not possible to detect the wall effect by analysis of pressure fluctuations in the frequency, RP and RQA methods showed that contribution of meso structures in the bed hydrodynamics increases by increasing the bed diameter.
- The relationship between entropy and operating parameters (i.e., superficial gas velocity, settled bed height), particle properties (particle size, minimum fluidization velocity) and bed diameter, was presented as:

$$ENT = 1.2 \left(\frac{U_0 - U_{mf}}{U_{mf}} \right)^{0.045} \frac{D^{1.27}}{L^{0.43} d_s^{0.46}}$$

- This entropy can be possibly used to improve the Glicksman's method of scaling. The entropy contains basic information of the system and might better reflect the fluidized bed hydrodynamics than the initial aspect ratio.

References

- [1] M. Rudisuli, T.J. Schildhauer, S.M.A. Biollaz, J.R. van Ommen, Scale-up of bubbling fluidized bed reactors - a review, *Powder Technol.* 217 (2012) 21–38.
- [2] M.L.M. van der Stappen, *Chaotic Hydrodynamics of Fluidized Beds*, Delft University of Technology, 1996.
- [3] F. Johnsson, R.C. Zijerveld, J.C. Schouten, C.M. van den Bleek, B. Leckner, Characterization of fluidization regimes by time-series analysis of pressure fluctuations, *Int. J. Multiph. Flow* 26 (2000) 663–715.
- [4] J.C. Schouten, C.M. van den Bleek, Monitoring the quality of the fluidization using the short-term predictability of pressure fluctuations, *AIChE J.* 44 (1998) 48–60.
- [5] S. Sasic, B. Leckner, F. Johnsson, Characterization of fluid dynamics of fluidized beds by analysis of pressure fluctuations, *Prog. Energy Combust. Sci* 33 (2007) 453–496.
- [6] J.R. van Ommen, J. van der Schaaf, J.C. Schouten, B.G.M. van Wachem, M.O. Coppens, C.M. van den Bleek, Optimal placement of probes for dynamic pressure measurements in large-scale fluidized beds, *Powder Technol.* 139 (2004) 264–276.
- [7] M. Abbasi, R. Sotudeh-Gharebagh, N. Mostoufi, M.J. Mahjoob, Non-intrusive monitoring of bubbles in a gas–solid fluidized bed using vibration signature analysis, *Powder Technol.* 196 (2009) 278–285.
- [8] M. Abbasi, R. Sotudeh-Gharebagh, N. Mostoufi, R. Zarghami, M. Mahjoob, Non intrusive characterisation of fluidised bed hydrodynamics using vibration signature analysis, *AIChE J.* 56 (2009) 597–603.
- [9] H. Azizpour, R. Sotudeh-Gharebagh, R. Zarghami, M. Abbasi, N. Mostoufi, M.J. Mahjoob, Characterization of gas–solid fluidized bed hydrodynamics by vibration signature analysis, *Int. J. Multiph. Flow* 37 (2011) 788–793.
- [10] D. Vervloet, J. Nijenhuis, J.R. van Ommen, Monitoring a lab-scale fluidized bed dryer: a comparison between pressure transducers, passive acoustic emissions and vibration measurements, *Powder Technol.* 197 (2010) 36–48.
- [11] N. Salehi-Nik, R. Sotudeh-Gharebagh, N. Mostoufi, R. Zarghami, M.J. Mahjoob, Determination of hydrodynamic behavior of gas–solid fluidized beds using statistical analysis of acoustic emissions, *Int. J. Multiph. Flow* 35 (2009) 1011–1016.
- [12] F. Karimi, R. Sotudeh-Gharebagh, R. Zarghami, M. Abbasi, N. Mostoufi, Conditional monitoring of moisture content in a fluidized bed dryer by the acoustic emission signature, *Korean J. Chem. Eng.* 29 (5) (2012) 595–600.
- [13] N. Yutani, N. Ototake, L.T. Fan, Stochastic analysis of fluctuations in the local void fraction of a gas–solids fluidised bed, *Powder Technol.* 48 (1986) 31–38.
- [14] J.R. van Ommen, S. Sasic, J. van der Schaaf, S. Gheorghiu, F. Johnsson, M.O. Coppens, Time-series analysis of pressure fluctuations in gas–solid fluidized beds - a review, *Int. J. Multiph. Flow* 37 (2011) 403–428.
- [15] J. van der Schaaf, J.R. van Ommen, F. Takens, J.C. Schouten, C.M. van den Bleek, Similarity between chaos analysis and frequency analysis of pressure fluctuations in fluidized beds, *Chem. Eng. Sci.* 59 (2004) 1829–1840.
- [16] N. Marwan, M. Carmen Romano, M. Thiel, J. Kurths, Recurrence plots for the analysis of complex systems, *Phys. Rep.* 438 (2007) 237–329.
- [17] M. Tahmasebpour, R. Zarghami, R. Sotudeh-Gharebagh, N. Mostoufi, Study of transition velocity from bubbling to turbulent fluidization by recurrence plots analysis on pressure fluctuations, *Can. J. Chem. Eng.* 91 (2013) 368–375.
- [18] M. Tahmasebpour, R. Zarghami, R. Sotudeh-Gharebagh, N. Mostoufi, Characterization of various structures in gas–solid fluidized beds by recurrence quantification analysis, *Particuology* 11 (2013) 647–656.
- [19] B. Babaei, R. Zarghami, H. Sedighikamal, R. Sotudeh-Gharebagh, N. Mostoufi, Investigating the hydrodynamics of gas–solid bubbling fluidization using recurrence plot, *Adv. Powder Technol.* 23 (2012) 380–386.
- [20] L.R. Glicksman, M.R. Hyre, P.A. Farrell, Dynamic similarity in fluidization, *Int. J. Multiph. Flow* 20 (1994) 331–386.
- [21] M.L.M. van der Stappen, J.C. Schouten, C.M. van den Bleek, Application of deterministic chaos theory in understanding the fluid dynamic behavior of gas–solid fluidization, *AIChE Symposium* 89 (1993) 91–102.
- [22] J.P. Eckmann, S.O. Kamphorst, D. Ruelle, Recurrence plots of dynamical systems, *Europhys. Lett.* 5 (9) (1987) 973–977.
- [23] T.K. March, S.C. Chapman, R.O. Dendy, Recurrence plot statistics and the effect of embedding, *Physica D* 200 (2005) 171–184.
- [24] S. Mallat, A theory for multi-resolution signal decomposition: the wavelet representation, *IEEE Trans. Pattern Anal. Mach. Intell.* 11 (1989) 674–693.
- [25] G.B. Zhao, Y.R. Yang, Multiscale resolution of fluidized-bed pressure fluctuations, *AIChE J.* 49 (2003) 869–882.
- [26] J. Li, M. Kwauk, *Particle-Fluid Two-Phase Flow: the Energy-Minimization Multi-scale Method*, Metallurgical Industry Press, Beijing, 1994.
- [27] B. Wu, A. Kantzas, C.T. Bellehumeur, Z. He, S. Kryuchkov, Multiresolution analysis of pressure fluctuations in gas–solids fluidized bed: application to glass beads and polyethylene powder systems, *Chem. Eng. J.* 131 (2007) 23–33.
- [28] M. Tahmasebpour, R. Zarghami, R. Sotudeh-Gharebagh, N. Mostoufi, Characterization of fluidized beds hydrodynamics by recurrence quantification analysis and wavelet transform, *Int. J. Multiph. Flow* 69 (2015) 31–41.
- [29] T.M. Knowlton, S.B.R. Karri, A. Issangya, Scale-up of fluidized-bed hydrodynamics, *Powder Technol.* 150 (2005) 72–77.
- [30] P.D. Welch, The use of a fast Fourier transform for the estimation of power spectra, *IEEE Trans. Audio Electroacoustics* AU-15 (1967) 70–73.